NEW YORK UNIVERSITY
INSTITUTE OF MATHEMATICAL SCIENCES
LIBRARY
25 Waverly Place, New York 3, N. Y.

AFOSR-TN-60-293

NEW YORK UNIVERSITY
Institute of Mathematical Sciences
Division of Electromagnetic Research

RESEARCH REPORT No. HT-5

Equation of State and Phase Transition of the Spherical Lattice Gas

WALTER PRESSMAN and JOSEPH B. KELLER

Contract No. AF 49(638)-341
Project No. 47501

FEBRUARY, 1960

NEW YORK UNIVERSITY
INSTITUTE OF MATHEMATICAL SCIENCES

HT-5
c.1

NEW YORK UNIVERSITY
Institute of Mathematical Sciences
Division of Electromagnetic Research

Research Report No. HT-5

Equation of State and Phase Transition of the Spherical Lattice Gas

Walter Pressman and Joseph B. Keller

Walter Pressman
Walter Pressman

Joseph B. Keller
Joseph B. Keller

Morris Kline
Morris Kline
Director

February, 1960

Qualified requestors may obtain copies of this report from the Arlington Hall Station, Arlington 12, Virginia. Department of Defense contractors must be established for ASTIA services, or have their 'need to know' certified by the cognizant military agency of their project.

Abstract

The spherical lattice gas is a modification of the ordinary lattice gas in which the occupation number of each cell is permitted to be any real number rather than ± 1. However the sum of squares of the occupation numbers is required to equal the number of cells. This permits one to evaluate the partition function by integrating over the surface of a certain sphere rather than by summing over lattice points on that surface. The partition function and the equation of state of the gas are evaluated in this way. It is found that in three dimensions the gas condenses, but not in one or two dimensions. Graphs of the phase transition curve and of the isotherms in three, two and one dimensions are presented.

The analytical work is simplified by taking advantage of the relationship between the properties of the lattice gas and of the Ising model of a ferromagnet. This relationship, demonstrated by C.N. Yang and T.D. Lee[1] for the ordinary lattice gas and Ising model, also applies to the spherical lattice gas and the spherical model of a ferromagnet. The properties of the latter have been evaluated by T.H. Berlin and M. Kac[2]. Graphs of the isotherms of the spherical model of the magnet, which were found in the course of the work, are also presented.

Table of Contents

	Page
1. Introduction	1
2. Basic formulas	2
3. The one-dimensional spherical lattice gas	7
4. The two-dimensional spherical lattice gas	9
5. The three-dimensional spherical lattice gas	11
6. Final remarks	14

1. Introduction.

The spherical lattice gas is a simplified model of a gas. We introduce it because we can deduce its equation of state statistical mechanically. We find that it undergoes phase transition in three dimensions, although not in one or two dimensions. We also find that its isotherms and transition curve, shown in Figure 9 are in qualitative agreement with experimental curves. However they exhibit a physically unreasonable negative pressure at very large and very small specific volumes. This can be traced to an inadequacy of the model for such specific volumes.

The ordinary lattice gas is defined by first dividing the volume V, which the gas occupies, into V identical cells (e.g. cubes), each of unit volume. The potential energy of interaction between two molecules of the gas is defined to be infinite if they occupy the same cell, to be $-4J < 0$ if they occupy cells which are nearest neighbors, and to be zero otherwise. Thus at most one particle can occupy each cell. Therefore the distribution of particles can be described by the V coordinates $\sigma_1, \sigma_2, \ldots, \sigma_V$ where $\sigma_i = +1$ if cell i is occupied and $\sigma_i = -1$ if it is not. We define the spherical lattice gas by permitting each σ_i to have any real value, but requiring that the σ_i lie on the sphere

$$\sum_{i=1}^{V} \sigma_i^2 = V \qquad (1)$$

Then the grand partition function Q_{SG} of the spherical lattice gas is obtained from that for the ordinary lattice gas by replacing sums over lattice points which lie on the sphere (1) by integrals over that sphere.

We were led to introduce the spherical lattice gas by the work of C. N. Yang and T. D. Lee [1] and that of T. H. Berlin and M. Kac [2]. Yang and Lee showed that Q_G, the grand partition function of the ordinary lattice gas, could be expressed in terms of Q_I, the partition function of the Ising model of ferromagnetism in a magnetic field H. But Q_I has not been evaluated for a three dimensional magnet nor for a two dimensional one with $H \neq 0$, although the spontaneous magnetization is known as a function of temperature in the two dimensional case. Therefore the phase transition curve of the two dimensional lattice gas could be determined, but not the isotherms, while nothing could be found for the three dimensional case.

Berlin and Kac introduced the spherical Ising model, which is related to the ordinary Ising model as the spherical lattice gas is to the ordinary lattice gas. They were able to evaluate its partition function Q_{SI} for any value of H in one, two and three dimensions. It exhibits spontaneous magnetization in three dimensions but not in one or two dimensions.

We noticed that the method of Berlin and Kac could be used to evaluate the grand partition function of the spherical lattice gas. We also noticed that Q_{SG} is related to Q_{SI} in the same way that Q_G is related to Q_I. Therefore we could actually use their results to obtain the value of Q_{SG}.

In the course of our analysis of the isotherms and transition curve of the spherical lattice gas, we were led to examine the magnetization curves and spontaneous magnetization of the spherical Ising model. Therefore these curves are also included.

2. Basic formulas.

The grand partition function of the lattice gas is [3, p.384]

$$\begin{aligned} Q_G(V,\mathcal{J},y) = \sum_{\sigma_1=\pm 1} \cdots \sum_{\sigma_V=\pm 1} \exp\left[\frac{\mathcal{J}}{2} \sum_{i,j=1}^{V} a_{ij}\sigma_i\sigma_j\right] \exp\Big[(c\,\mathcal{J} + \tfrac{1}{2}\ln y) \qquad (2) \\ \times \sum_{j=1}^{V} \sigma_j\Big] \exp\left[\tfrac{1}{2}(c\,\mathcal{J} + \ln y)V\right] . \end{aligned}$$

Here σ_i equals +1 if cell i is occupied by a particle and -1 if it is not. We note that the σ_i satisfy (1) and

$$\sigma_i^2 = 1 \ . \tag{3}$$

The constant $\mathcal{J}$ is defined in terms of Boltzmann's constant k and the absolute temperature T by

$$\mathcal{J} = J/kT \ . \tag{4}$$

The quantity a_{ij} equals +1 if cells i and j are nearest neighbors and is zero otherwise, while c is the number of nearest neighbors of a cell. For cubic cells in one, two, and three dimensions c equals two, four, and six respectively. The fugacity is denoted by y.

From the definition of the spherical lattice gas, its grand partition function is

$$Q_{SG}(V, \mathcal{J}, y) = \underset{\sum \sigma_i^2 = V}{\int \cdots \int} d\sigma_1 \ldots d\sigma_V \exp\left[\frac{\mathcal{J}}{2} \sum_{i,j=1}^{V} a_{ij}\sigma_i\sigma_j\right] \exp\left[(c\mathcal{J} + \frac{1}{2}\ln y) \times \sum_{j=1}^{V} \sigma_j\right] \exp\left[\frac{1}{2}(c\mathcal{J} + \ln y)V\right] \ . \tag{5}$$

The partition function for the Ising model of ferromagnetism is [3,p.353]

$$Q_I(N, \mathcal{J}, \mathcal{H}) = \sum_{\sigma_1 = \pm 1} \cdots \sum_{\sigma_N = \pm 1} \exp\left[\frac{\mathcal{J}}{2} \sum_{i,j=1}^{N} a_{ij}\sigma_i\sigma_j + \mathcal{H} \sum_{j=1}^{N} \sigma_j\right] \ . \tag{6}$$

In (6) N is the total number of lattice sites and

$$\mathcal{H} = \frac{\mu_o H}{kT} \ . \tag{7}$$

Here μ_o is the magnetic moment per particle.

The partition function for the spherical model of ferromagnetism is [2,p.827]

$$Q_{SI}(N, \mathcal{J}, \mathcal{H}) = \underset{\sum \sigma_i^2 = N}{\int \cdots \int} d\sigma_1 \ldots d\sigma_N \exp\left[\frac{\mathcal{J}}{2} \sum_{i,j=1}^{N} a_{ij}\sigma_i\sigma_j + \mathcal{H} \sum_{j=1}^{N} \sigma_j\right] . \tag{8}$$

In (2) let us replace V by N and set

$$\ln y = 2[\mathcal{H} - c\mathcal{J}] .$$

Then by comparing (2) with (6) we obtain the following relationship, first obtained by Yang,

$$Q_G\left(N, \mathcal{J}, \exp\left[2(\mathcal{H} - c\mathcal{J})\right]\right) = \exp\left[\mathcal{H} - \frac{1}{2} c\mathcal{J}\right] Q_I(N, \mathcal{J}, \mathcal{H}) . \tag{9}$$

Upon comparing (5) and (8) we obtain the corresponding relation for the spherical models,

$$Q_{SG}\left(N, \mathcal{J}, \exp\left[2(\mathcal{H} - c\mathcal{J})\right]\right) = \exp\left[\mathcal{H} - \frac{1}{2} c\mathcal{J}\right] Q_{SI}(N, \mathcal{J}, \mathcal{H}) . \tag{10}$$

From either (9) or (10) it follows that [3,p.384] the thermodynamic properties of the lattice gas are related to those of the magnet. These relations are the same for the spherical and the original models. They are

$$p^*(\mathcal{J}, \mathcal{H}) = \frac{F + \mathcal{H}}{\mathcal{J}} - \frac{c}{2} , \tag{11}$$

$$v(\mathcal{J}, \mathcal{H}) = \frac{2}{1 + \mathfrak{m}} . \tag{12}$$

Here $p^* = p/J$ where p is the pressure of the gas, v is its specific volume, and $\mathfrak{m} = M/\mu_o$ where M is the magnetization of the magnet. F, the limiting free energy per particle of the magnet, is defined by

$$F(\mathcal{H}, \mathcal{J}) = \lim_{N \to \infty} \frac{1}{N} \ln Q . \tag{13}$$

Here Q denotes either Q_I or Q_{SI}. $\mathfrak{m}$ is given by

$$\mathfrak{m}(\mathcal{H},\mathcal{J}) = \frac{\partial F}{\partial \mathcal{H}} \,. \tag{14}$$

Equations (11) and (12) are the parametric form of the equation of state of either the lattice gas or the spherical lattice gas. The parameter is $\mathcal{H}$, which ranges from minus infinity to plus infinity.

To obtain the equation of state of the spherical lattice gas we must insert $F(\mathcal{H},\mathcal{J})$, the limiting free energy per particle of the spherical Ising model, into (11) and (14) and then use (14) in (12). For a simple cubic lattice in n dimensions ($n = 1,2,3$), Berlin and Kac[2] have evaluated this free energy which we denote by $F_n(\mathcal{H},\mathcal{J})$. They obtain

$$F_n(\mathcal{H},\mathcal{J}) = \frac{1}{2}\ln\left(\frac{\pi}{\mathcal{J}}\right) - \frac{1}{2} f_n(z) + \mathcal{J} z + \frac{\mathcal{H}^2}{4\mathcal{J}(z-n)} \,. \tag{15}$$

In (15) we have omitted an additive constant which occurs in [2] due to multiplication of Q_{SI} by a normalization factor. Here z is a real positive solution of the equation

$$2\mathcal{J} = \frac{\mathcal{H}^2}{2\mathcal{J}(z-n)^2} + \frac{df_n(z)}{dz} \,. \tag{16}$$

The function $f_n(z)$ is defined by

$$f_n(z) = \frac{1}{(2\pi)^n} \int_0^{2\pi} \cdots \int_0^{2\pi} dw_1 \ldots dw_n \ln\left[z - \sum_{j=1}^{n} \cos w_j\right] \,. \tag{17}$$

It will prove convenient later to note that (16) implies $dF_n(z)/dz = 0$ and that z is an even function of $\mathcal{H}$. Then (15) shows that F_n is also an even function of $\mathcal{H}$.

The equation of state of the spherical Ising model of a magnet is obtained by inserting (15) into (14). It is

$$\mathfrak{m}(\mathcal{H},\mathcal{J}) = \frac{\mathcal{H}}{2\mathcal{J}(z-n)} \,. \tag{18}$$

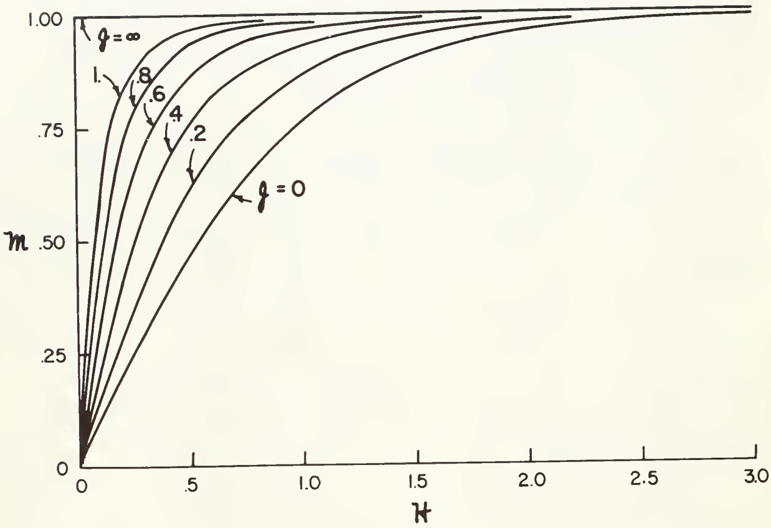

Fig. 1 - Isotherms of the one-dimensional Ising model of a ferromagnet. The curves, based on equation (20), give the normalized magnetization $\mathcal{M} = M/\mu_0$ as a function of the normalized external field $\mathcal{H} = H/kT$ for constant values of $\mathcal{J} = J/kT$. Since $\mathcal{M}$ is an odd function of $\mathcal{H}$, only the non-negative values of $\mathcal{H}$ are shown.

From (18) we see that $\mathcal{M}$ is an odd function of $\mathcal{H}$. In the following sections we shall examine the equation of state of the spherical lattice gas and of the spherical Ising model in detail on the basis of the above equations.

In order to compare the properties of the spherical lattice gas with those of the lattice gas, we must determine the properties of the latter. We can do this in the one dimensional case. The limiting free energy per particle of the one dimensional Ising model F_{1I}, is [3,p.385]

$$F_{1I}(\mathcal{H},\mathcal{J}) = \ln\left[e^{\mathcal{J}}\cosh\mathcal{H} + \left(e^{2\mathcal{J}}\sinh^2\mathcal{H} + e^{-2\mathcal{J}}\right)^{1/2}\right] . \tag{19}$$

Upon substituting (19) into (14) we obtain

$$\mathcal{M}_{1I}(\mathcal{H},\mathcal{J}) = \left(\sinh^2\mathcal{H} + e^{-4\mathcal{J}}\right)^{-1/2} \sinh\mathcal{H} . \tag{20}$$

(This formula is misprinted in [3].) From (20) we deduce, omitting the subscripts

$$\mathcal{M}(\mathcal{H},0) = \tanh\mathcal{H} \tag{21a}$$

$$\mathcal{M}(\mathcal{H},\infty) = 1 \qquad \mathcal{H} > 0 \tag{21b}$$

$$\mathcal{M}(0,\mathcal{J}) = 0 \qquad \mathcal{J} < \infty \tag{21c}$$

$$\mathcal{M}(\infty,\mathcal{J}) = 1 . \tag{21d}$$

Equation (21c) demonstrates the well known fact that spontaneous magnetization does not occur in the one-dimensional Ising model. Magnetization curves based on (20) are shown in Figure 1. Less complete graphs are given in [3].

Upon substituting (19) into (11) and (20) into (12) we obtain the equation of state of the one dimensional lattice gas in parametric form

$$p^* = \frac{1}{\mathcal{J}}\left\{\ln\left[e^{\mathcal{J}}\cosh\mathcal{H} + \left(e^{2\mathcal{J}}\sinh^2\mathcal{H} + e^{-2\mathcal{J}}\right)^{1/2} + \mathcal{H}\right]\right\} - 1 , \tag{22}$$

$$v = 2\left[1 + \left(\sinh^2\mathcal{H} + e^{-4\mathcal{J}}\right)^{-1/2}\sinh\mathcal{H}\right]^{-1} . \tag{23}$$

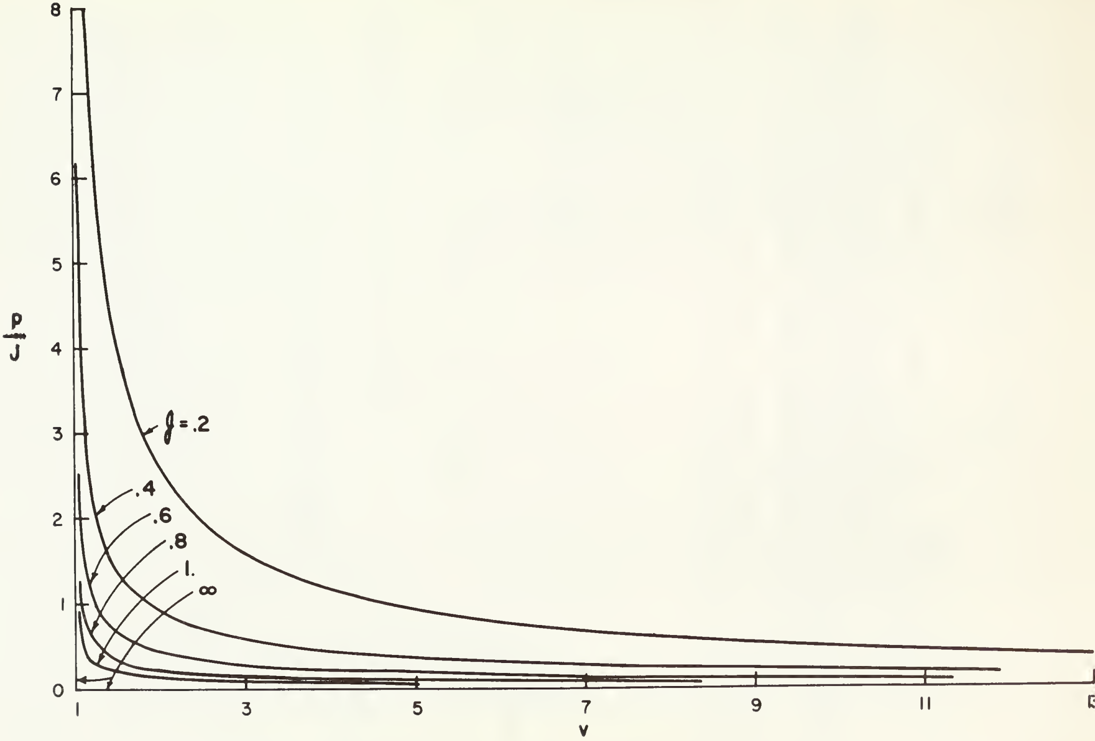

Fig.2-Isotherms of the one-dimensional lattice gas based on equations (22) and (23). The curves show the normalized pressure $p^* = p/J$ as a function of specific volume v for various values of $\mathcal{J} = J/kT$.

Isotherms of the one - dimensional lattice gas based on (22) and (23) are shown in Figure 2. We see from (23) that as $\mathcal{H}$ varies from + ∞ to - ∞, v varies continuously and hence no phase transition occurs. We also obtain easily the following values, listed in Table I

Table 1

$\mathcal{H}$	$\mathfrak{m}$	v	p^*
$+\infty$	$+1$	1	$\sim \frac{2\mathcal{H}}{\mathcal{J}} \to +\infty$
0	0	2	$\frac{1}{\mathcal{J}} \ln(2 \cosh \mathcal{J}) - 1$
$-\infty$	-1	$+\infty$	0

We see that the equations of state of the one-dimensional Ising model and of the one dimensional lattice gas are physically quite reasonable.

3. The one-dimensional spherical lattice gas.

Since the properties of the spherical lattice gas can be found in terms of those of the spherical Ising model, we shall first examine that model. Its equation of state is given by (16) and (18) which become, in one dimension,

$$2\mathcal{J} = \frac{\mathcal{H}^2}{2\mathcal{J}(z-1)^2} + \frac{1}{(z^2-1)^{1/2}} , \tag{24}$$

$$\mathfrak{m} = \frac{\mathcal{H}}{2\mathcal{J}(z-1)} . \tag{25}$$

From (24) and (25) we find that

$$\mathfrak{m}(\mathcal{H},0) = 2\mathcal{H}\left[1 + (1+4\mathcal{H}^2)^{1/2}\right]^{-1}, \tag{26a}$$

$$\mathfrak{m}(\mathcal{H},\infty) = 1 , \qquad \mathcal{H} > 0 , \tag{26b}$$

$$\mathfrak{m}(0,\mathcal{J}) = 0 , \qquad \mathcal{J} < \infty, \tag{26c}$$

$$\mathfrak{m}(\infty,\mathcal{J}) = 1 . \tag{26d}$$

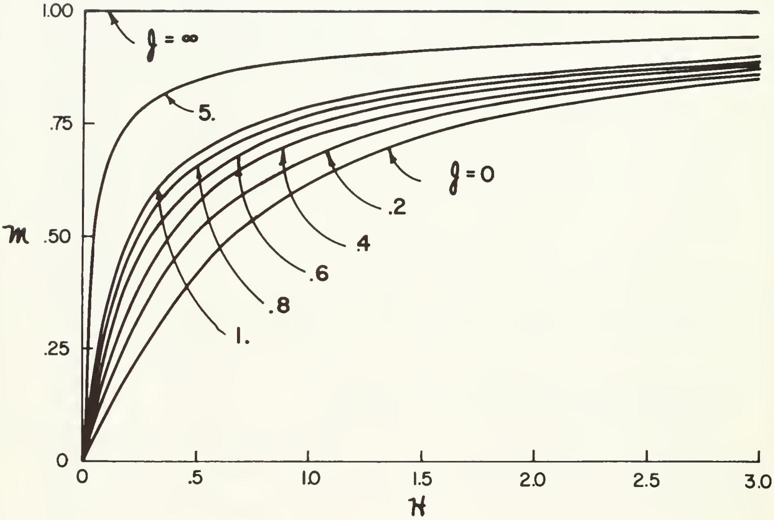

Fig. 3- Isotherms of the one-dimensional spherical model of a ferromagnet based on equations (24) and (25). The normalized magnetization $\mathcal{M} = M/\mu_0$ is shown as a function of the normalized external field $\mathcal{H} = H/kT$ for various constant values of $\mathcal{J} = J/kT$. These curves lie below the corresponding ones of the Ising model shown in Figure 1.

The proofs of these results are similar to, but simpler than, those given in Appendix B for the three dimensional case. Equation (26c) shows that spontaneous magnetization does not occur in this case. Magnetization curves of the spherical Ising model, based on (24) and (25), are shown in Figure 3. For a given $\mathcal{H}$ and $\mathcal{J}$, the magnetization of the spherical model is less than that of the Ising model (Figure 1).

From (11) and (15) we obtain for the spherical lattice gas in one dimension

$$p^{*}(\mathcal{J},\mathcal{H}) = \frac{F_1 + \mathcal{H}}{\mathcal{J}} - 1 \quad , \tag{28}$$

$$F_1(\mathcal{H},\mathcal{J}) = \frac{1}{2}\ln\left(\frac{\pi}{\mathcal{J}}\right) - \frac{1}{2}\ln\frac{1}{2}\left[z + (z^2-1)^{1/2}\right] + \mathcal{J}z + \frac{\mathcal{H}^2}{4\mathcal{J}(z-1)} \quad . \tag{29}$$

From (12) and (25) we obtain

$$v(\mathcal{J},\mathcal{H}) = 2\left[1 + \frac{\mathcal{H}}{2\mathcal{J}(z-1)}\right]^{-1} \quad . \tag{30}$$

Equations (28) - (30) express the equation of state of the one dimensional spherical lattice gas in terms of the parameter $\mathcal{H}$. The quantity z is defined as a root of (24). Isotherms of the one-dimensional spherical lattice gas based on (28) - (30) are shown in Figure 4. The method of computation used in preparing this and the subsequent figures is explained in Appendix A. Since spontaneous magnetization does not occur in the spherical magnet, phase transition does not occur in the spherical lattice gas. Much as in Appendix B we obtain the special results shown in Table 2.

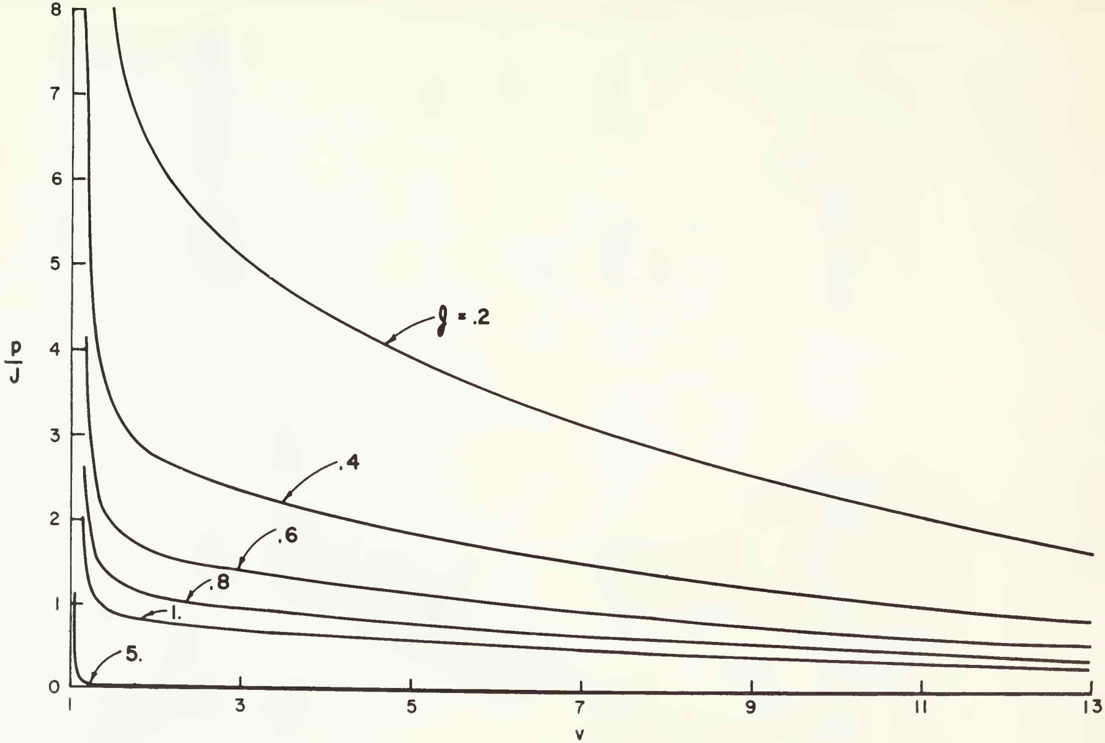

Fig.4 - Isotherms of the one-dimensional spherical lattice gas based on equations (28) - (30). The curves show the normalized pressure $p^* = p/J$ as a function of specific volume v for various values of $\mathcal{J} = J/kT$. Each isotherm crosses the axis $p^* = 0$ for a sufficiently large value of v indicating the inadequacy of the model for such large values of v.

Table 2

$\mathcal{H}$	$\mathfrak{m}$	v	p^*
$+\infty$	1	1	$\sim \frac{2\mathcal{H}}{\mathcal{J}} \to +\infty$
0	0	2	$\frac{1}{2\mathcal{J}}\left\{(1+4\mathcal{J}^2)^{1/2} - \ln \frac{1}{4\pi}\left[1+4\mathcal{J}^2)^{1/2}\right]\right\} -1$
$-\infty$	-1	$+\infty$	$\sim -\frac{\ln\|\mathcal{H}\|}{2\mathcal{J}} \to -\infty$

We note from the third line of the table that when v becomes large, p becomes negative. Furthermore for large v the isotherms corresponding to large values of $\mathcal{J}$ lie below those corresponding to smaller values of $\mathcal{J}$. This unphysical behavior of the equation of state for large v is due to the inadequacy of the spherical model in this limit.

4. The two-dimensional spherical lattice gas.

For n = 2, equations (16) and (18) for the spherical Ising model become

$$2\mathcal{J} = \frac{\mathcal{H}^2}{2\mathcal{J}(z-2)^2} + \frac{2}{\pi z} K\left(\frac{2}{z}\right), \tag{31}$$

$$\mathfrak{m}(\mathcal{H}, \mathcal{J}) = \frac{\mathcal{H}}{2\mathcal{J}(z-2)} . \tag{32}$$

In (31), K(a) is the complete elliptic integral of the first kind, $0 \leq a \leq 1$. From (31) and (32) we find that (26) is still valid for n = 2. This is shown as in Appendix B by using the facts that $K(0) = \pi/2$ and $K(1) = \infty$. From (26c) we see that spontaneous magnetization does not occur for the spherical Ising model when n = 2. The Ising model, however, does exhibit spontaneous magnetization when n = 2. Magnetization curves based on (31) and (32) are shown in Figure 5.

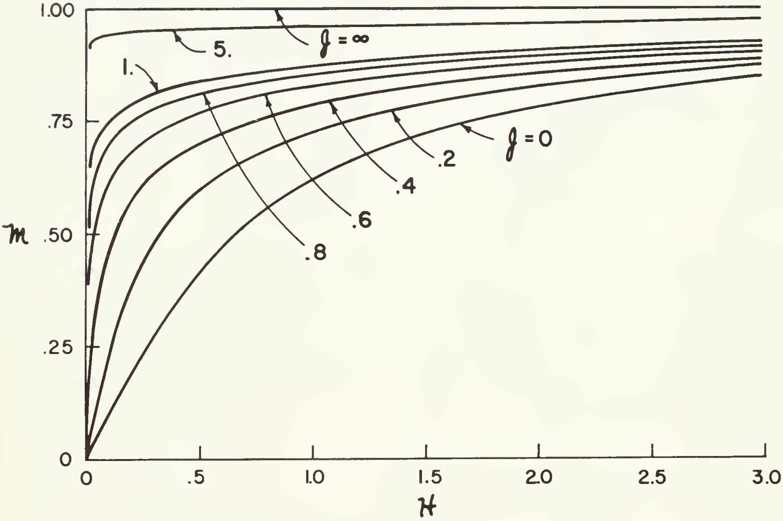

Fig.5 - Isotherms of the two-dimensional spherical model of a ferromagnet based on equations (31) and (32). The normalized magnetization $\mathcal{M} = M/\mu_0$ is shown as a function of the normalized external field $\mathcal{H} = H/kT$ for various constant values of $\mathcal{J} = J/kT$.

To obtain the equation of state of the spherical lattice gas in two dimensions, we set n = 2 in (11) and (15) which become

$$p^*(\mathcal{J},\mathcal{H}) = \frac{F_2 + \mathcal{H}}{\mathcal{J}} - 2 \;, \tag{34}$$

$$F_2(\mathcal{H},\mathcal{J}) = \frac{1}{2}\ln\frac{\pi}{\mathcal{J}} - \frac{1}{2}f_2(z) + \mathcal{J}z + \frac{\mathcal{H}^2}{4\mathcal{J}(z-2)} \;. \tag{35}$$

Here $f_2(z)$ is defined by

$$f_2(z) = \frac{1}{(2\pi)^2}\int_0^{2\pi}\int_0^{2\pi} dw_1 dw_2 \ln\left[z - \cos w_1 - \cos w_2\right] \;.$$

Upon integrating once, $f_2(z)$ becomes

$$f_2(z) = \frac{1}{\pi}\int_0^{\pi} dw \ln\frac{1}{2}\left\{(z - \cos w) + \left[(z-\cos w)^2 - 1\right]^{1/2}\right\} \;. \tag{36}$$

From (12) and (32) we obtain

$$v(\mathcal{J},\mathcal{H}) = 2\left[1 + \frac{\mathcal{H}}{2\mathcal{J}(z-2)}\right]^{-1} \;. \tag{37}$$

Isotherms of the two-dimensional spherical lattice gas based on (34)-(37) are shown in Figure 6. From (26), (34) and (37), by considerations like those in Appendix B, we obtain the special results in Table 3.

Table 3

$\mathcal{H}$	m	v	p^*
$+\infty$	1	1	$\frac{2\mathcal{H}}{\mathcal{J}} \to +\infty$
0	0	2	$\frac{1}{2\mathcal{J}}\left\{\ln\frac{\pi}{\mathcal{J}} - f_2(z_m) + \mathcal{J}z_m\right\} - 2$
$-\infty$	-1	$+\infty$	$-\frac{\ln\lvert\mathcal{H}\rvert}{2\mathcal{J}} \to -\infty$

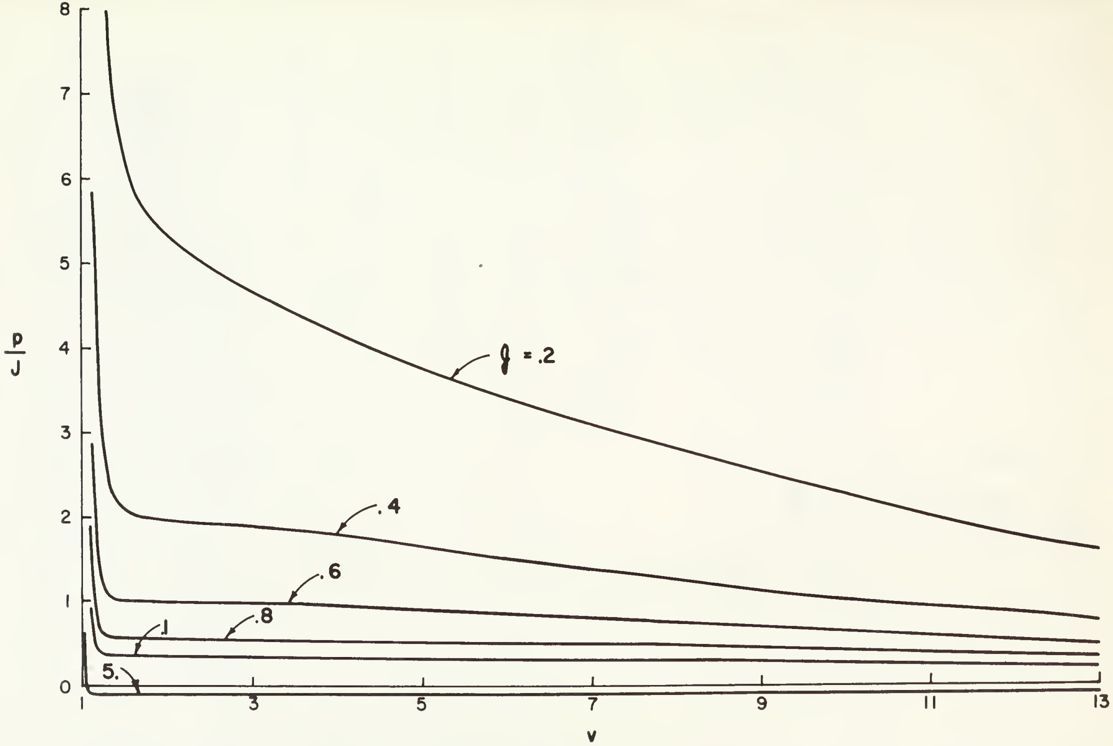

Fig.6 - Isotherms of the two-dimensional spherical lattice gas based on equations (34) - (37). The curves show the normalized pressure $p^* = p/J$ as a function of specific volume v for various values of $\mathcal{J} = J/kT$. Each isotherm crosses the axis $p^* = 0$ for a sufficiently large value of v indicating the inadequacy of the model for such large values of v.

Here z_m is the solution of equation (3) in Appendix C. We see from the third line of the table that for large v the behavior of the two dimensional spherical lattice gas is unphysical, just as in the one dimensional case.

5. The three-dimensional spherical lattice gas.

In three dimensions (16) and (18) for the spherical Ising model become

$$2\mathcal{J} = \frac{\mathcal{H}^2}{2\mathcal{J}(z-3)^2} + \frac{df_3(z)}{dz} \quad , \tag{38}$$

$$\mathfrak{m}(\mathcal{H},\mathcal{J}) = \frac{\mathcal{H}}{2\mathcal{J}(z-3)} \quad . \tag{39}$$

In (38) df_3/dz is given by

$$\frac{df_3(z)}{dz} = \frac{1}{(2\pi)^3} \int_0^{2\pi}\int_0^{2\pi}\int_0^{2\pi} \frac{dw_1 dw_2 dw_3}{z - \cos w_1 - \cos w_2 - \cos w_3} \tag{40}$$

$$= \frac{1}{\pi^2} \int_0^{\pi} dw\left(\frac{2}{z - \cos w}\right) K\left(\frac{2}{z - \cos w}\right) \quad .$$

In Appendix B we show that

$$\mathfrak{m}(\mathcal{H},0) = 2\mathcal{H}\left[1 + (1 + 4\mathcal{H}^2)^{1/2}\right]^{-1} \tag{41a}$$

$$\mathfrak{m}(\mathcal{H},\infty) = 1 \qquad \mathcal{H} > 0 \tag{41b}$$

$$\mathfrak{m}(0+,\mathcal{J}) = \left(1 - \frac{\mathcal{J}_c}{\mathcal{J}}\right)^{1/2} \qquad \text{for } \mathcal{J} > \mathcal{J}_c = .2527\ldots \tag{41c}$$

$$\mathfrak{m}(0,\mathcal{J}) = 0 \qquad \mathcal{J} < \mathcal{J}_c \tag{41d}$$

$$\mathfrak{m}(\infty,\mathcal{J}) = 1 \quad . \tag{41e}$$

Equations (41c) and (41d) show that spontaneous magnetization occurs for $\mathcal{J} > \mathcal{J}_c$.

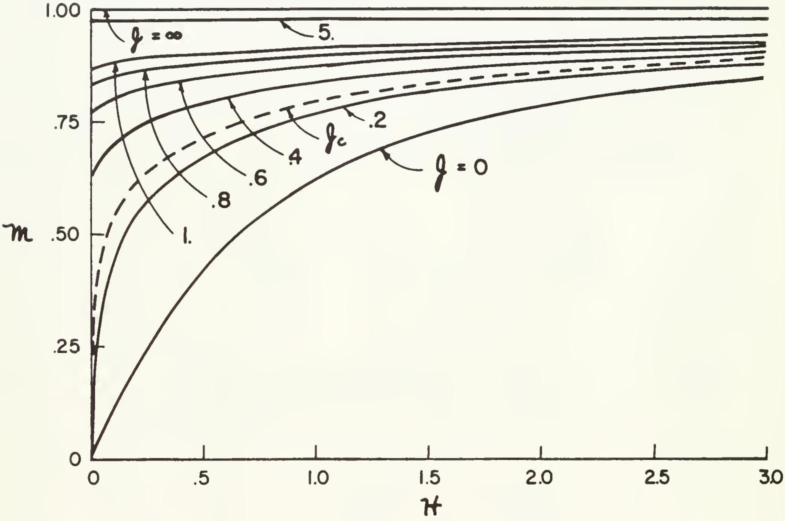

Fig.7 - Isotherms of the three-dimensional spherical model of a ferromagnet based on equations (38) - (40). The normalized magnetization $\mathcal{M} = M/\mu_o$ is shown as a function of the normalized external field $\mathcal{H} = H/kT$ for various constant values of $\mathcal{J} = J/kT$. Spontaneous magnetization occurs for $\mathcal{J} > \mathcal{J}_c = .2527$. This is shown by the fact that for such values of $\mathcal{J}$, the magnetization is different from zero for $\mathcal{H} = 0$.

In Appendix D it is proved that

$$\left.\frac{d\mathcal{M}}{d\mathcal{H}}\right|_{\mathcal{H}=0} = 1 \qquad \mathcal{J} = 0 \tag{42}$$

$$\left.\frac{d\mathcal{M}}{d\mathcal{H}}\right|_{\mathcal{H}=0} = \frac{1}{2\mathcal{J}(z_m-3)} \qquad 0 < \mathcal{J} < \mathcal{J}_c \tag{43}$$

$$\left.\frac{d\mathcal{M}}{d\mathcal{H}}\right|_{\mathcal{H}=0} = \infty \qquad \mathcal{J} > \mathcal{J}_c \tag{44}$$

Here z_m is the solution of equation (4) of Appendix C. Magnetization curves based on (38) - (41) are shown in Figure 7. The spontaneous magnetization curve based on (41c) is shown in Figure 8.

The equation of state of the three dimensional spherical lattice gas is now obtained by setting n = 3 in (11) and (15) which become

$$p^*(\mathcal{J},\mathcal{H}) = \frac{F_3 + \mathcal{H}}{\mathcal{J}} - 3 \ , \tag{45}$$

$$F_3(\mathcal{H},\mathcal{J}) = \frac{1}{2}\ln\frac{\pi}{\mathcal{J}} - \frac{1}{2}f_3(z) + \mathcal{J}z + \frac{\mathcal{H}^2}{4\mathcal{J}(z-3)} \quad . \tag{46}$$

Here $f_3(z)$ is given by

$$f_3(z) = \frac{1}{(2\pi)^3}\int_0^{2\pi}\int_0^{2\pi}\int_0^{2\pi} dw_1 dw_2 dw_3 \ln(z - \cos w_1 - \cos w_2 - \cos w_3) \,. \tag{47}$$

Equations (12) and (39) yield

$$v(\mathcal{J},\mathcal{H}) = 2\left[1 + \frac{\mathcal{H}}{2\mathcal{J}(z-3)}\right]^{-1} \quad . \tag{48}$$

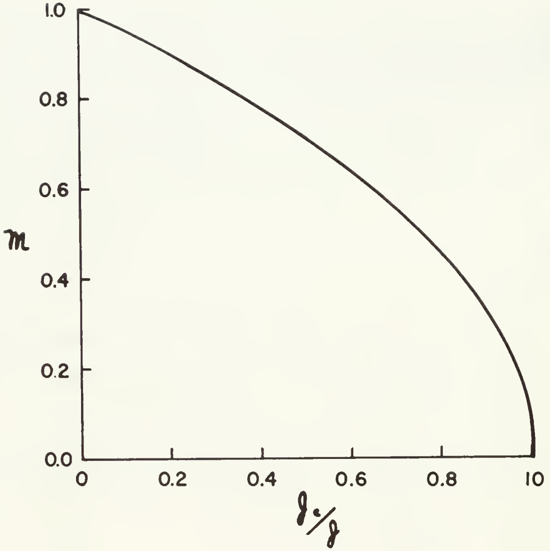

Fig.8 - Spontaneous magnetization of the three-dimensional spherical model of a ferromagnet based on equation (41c). The ordinate is the limiting value of the magnetization $\mathcal{M}(\mathcal{H},\mathcal{J})$ as $\mathcal{H}$ tends to zero through positive values. It is just the intercept of the isotherms with the axis $\mathcal{H} = 0$ in Figure 7. The abcsissa is $\mathcal{J}_c/\mathcal{J}$.

From (41), (45) and (48) we derive, in Appendix C, the entries of Table 4. In this table z_m is the solution of equation (4) of Appendix C, while v_L and v_G are determined by the equations

$$v_L = 2\left[1 + M(0+, \vartheta)\right]^{-1} \tag{49}$$

$$\frac{1}{v_L} + \frac{1}{v_G} = 1 \ . \tag{50}$$

For very small and very large v, the isotherms behave as they do in the one- and two-dimensional cases. However for $\vartheta > \vartheta_c$, a discontinuity occurs in the p^*, v curves at the parameter value $\mathcal{H} = 0$. At this value we obtain two different specific volumes for each p^*. We designate the smaller v_L to indicate the value at which the liquid begins to vaporize. The larger we call v_G, which is the specific volume at which the gas begins to liquify. The jump in specific volume is

$$v_G - v_L = \frac{4M(0+, \vartheta)}{1-M^2(0+, \vartheta)} \ . \tag{51}$$

We now eliminate ϑ between (45) and (49), obtaining

$$p^* = \frac{2}{\vartheta_c}\left(\frac{v_L-1}{v_L^2}\right)\left[\ln\left(\frac{v_L-1}{v_L^2}\right) + \ln\frac{4\pi}{\vartheta_c} - f_3(3)\right], \quad 1 \leq v_L \leq 2 \ . \tag{52}$$

Equation (52) defines that half of the phase transition curve, or boundary of the two phase region, in the p^*,v plane at which the liquid begins to vaporize. The other half of this curve is obtained by eliminating v_L from (52) by means of (50), which yields a relation between p^* and v_G. This is the half of the phase transition curve at which the gas begins to liquify. The maximum of p^* on this curve occurs at $v_L = v_G = 2$, where $\partial p^*/\partial v_L = \partial p^*/\partial v_G = 0$. It is

Table 4

$\mathcal{H}$		m	v	p^*
$+\infty$		$+1$	1	$\sim \frac{2\mathcal{H}}{g} \to +\infty$
$0\pm$	$(g < g_c)$	0	2	$\frac{1}{2g}\left[\ln\frac{\pi}{g} + 2g z_m - f_3(z_m)\right] -3$
$0+$	$(g > g_c)$	$+m(0+, g)$	v_L	$\frac{1}{2g}\left[\ln\frac{\pi}{g} - f_3(3)\right]$
$0-$	$(g > g_c)$	$-m(0+, g)$	v_G	
$-\infty$		-1	$+\infty$	$\sim -\frac{\ln\lvert\mathcal{H}\rvert}{2g} \to -\infty$

interesting to note that at the maximum $\partial^2 p / \partial v_L^2 = \partial^2 p / \partial v_G^2 \neq 0$. Thus the phase transition curve is not as flat at its maximum as is that of the two dimensional ordinary lattice gas. The phase transition curve or two phase boundary is shown as a dashed line in Figure 9.

In order to examine the isotherms of the three dimensional spherical lattice gas, we prove in Appendix D that

$$\left.\frac{dp^*}{dv}\right|_{v=2} = -(z_m - 3) \qquad \mathcal{J} < \mathcal{J}_c \tag{53}$$

$$\left.\frac{dp^*}{dv}\right|_{v=v_L, v_G} = 0 \qquad \mathcal{J} > \mathcal{J}_c\,. \tag{54}$$

From (54) we see that the isotherms meet the two-phase boundary with zero slope and that the compressibility is infinite at this boundary. The isotherms are shown in Figure 9. The horizontal line within the two phase region in that figure represents the discontinuity (51).

Although Figure 9 bears a marked qualitative resemblance to the p, v diagram of a real gas-liquid system, it is unrealistic for large $\mathcal{J}$ at small v and for all $\mathcal{J}$ at large v. This is shown by the small negative trough of the condensation curve for $1 \leq v \leq 2$ and by a corresponding one of the same depth but of infinite extent for large values of v.

6. Final remarks.

Our method of computation of the isotherms from (45) - (48) is described in Appendix A. In this computation for each $\mathcal{J}$, values were assigned to the two parameters z and $\mathcal{H}$, and corresponding values of p^* and v were computed. The values of $\mathcal{H}$ ranged from $-\infty$ to $+\infty$ and those of z ranged from z_m to $+\infty$. The minimum value z_m is determined in Appendix C as a root of equation (1) of that Appendix. We now wish to determine whether the isotherms can be continued

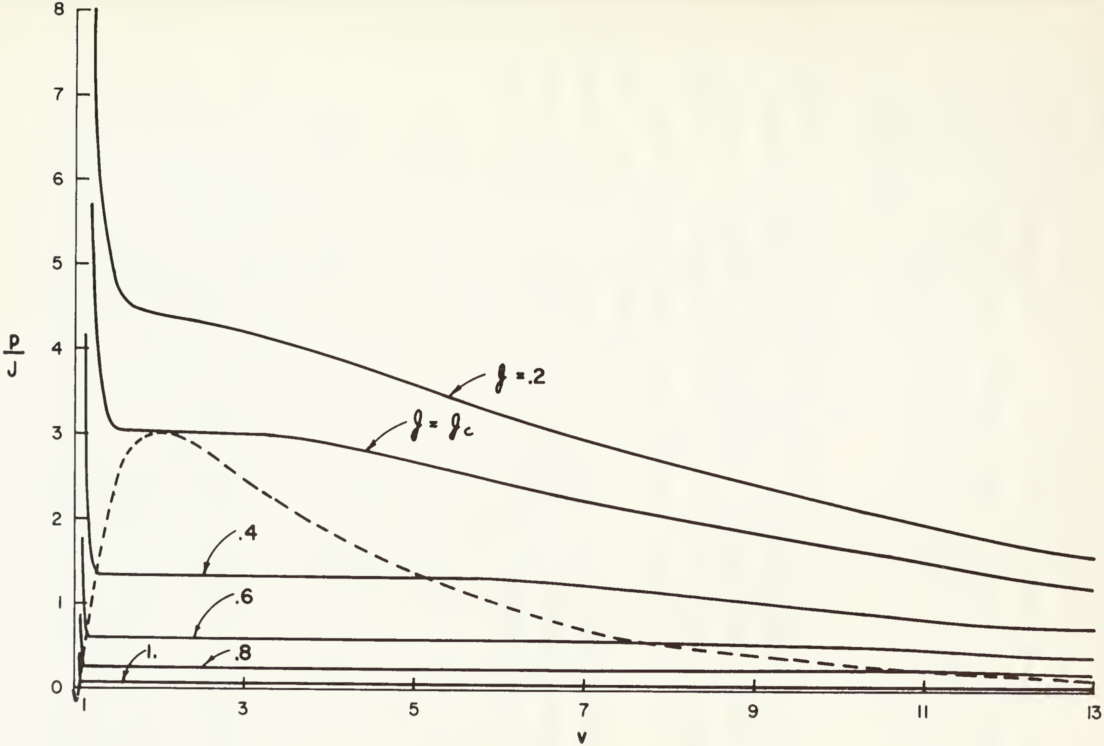

Fig.9 - Isotherms of the three-dimensional spherical lattice gas based on equations (45)-(48). The curves show the normalized pressure $p^* = p/J$ as a function of specific volume v for various values of $\mathcal{J} = J/kT$. Each isotherm crosses the axis $p^* = 0$ for a sufficiently large value of v indicating the inadequacy of the model for such large values of v. The dashed curve is the boundary of the two phase region. Half of it is given by (52) and the other half by (50) and (52). The horizontal part of each isotherm in the two phase region has been drawn to connect the end points of the two other portions of the isotherm. This horizontal part is not described by our equations, which do not yield any isotherms in this region.

beyond the two phase boundary by choosing $z < z_m$. If so, we wish to see if such a continuation has physical significance. In particular, does it yield metastable states?

We first consider the spherical Ising model and write (16) and (18) in the form

$$\mathcal{M}^2 = 1 - \frac{1}{2\mathcal{J}} \frac{df_n}{dz} \quad , \tag{55}$$

$$\mathcal{H} = 2\mathcal{J}(z - n)\mathcal{M} \ . \tag{56}$$

In one, two and three dimensions the following remarks apply. If $n < z < z_m$ it follows that $\frac{1}{2\mathcal{J}} \frac{df_n(z\ )}{dz} > 1$. Then (55) shows that $\mathcal{M}$ is imaginary. If $|z| < n$ then from (17) we find that $\frac{df_n}{dz}$ is infinite. Hence we need consider only $z \leq -n$.

From (17) we note that $\frac{df_n(z)}{dz}$ is an odd function of z. Therefore we replace z by -z in (55) and (56) and obtain

$$\mathcal{M}^2 = 1 + \frac{1}{2\mathcal{J}} \frac{df_n(z)}{dz} \ , \tag{57}$$

$$\mathcal{H} = -2\mathcal{J}\mathcal{M}(z + n), \qquad\qquad z > n \ . \tag{58}$$

Since $\frac{df_n}{dz}$ is finite and positive for $z > n$, (57) and (58) yield two real continuations for $\mathcal{M}$ and $\mathcal{H}$ since two values of the square root can be used in (57). According to (58), $\mathcal{M}$ and $\mathcal{H}$ have opposite signs for each solution, and from (57) $|\mathcal{M}| > 1$. Thus both of these continuations seem to be physically unrealistic.

We shall now consider the possibility of continuing the isotherms of the spherical lattice gas. First we consider the range $n < z < z_m$. Since $\mathcal{M}$ is imaginary in this range, we see from (12) that v will be complex. On the other hand, if $z < n$, (17) shows that $f_n(z)$ is complex. Then (15) and (11) show that

p^* is not real. Thus if z and $\mathcal{H}$ are real, there is no real continuation of the isotherms.

Next we shall show that when v, p* and $\mathcal{J}$ are all real then z and $\mathcal{H}$ must be real. To show this we first note that from (12), $\mathcal{M}$ is real if v is real. Then from (55) it follows that z is real. For if z were not real, by (17) df_n/dz would not be real and then (55) would show that $\mathcal{M}$ would not be real. Finally from (18), the reality of z and $\mathcal{M}$ imply that $\mathcal{H}$ is real. This result and that of the preceding paragraph show that, on the basis of our equations, there is no real continuation of the isotherms of the spherical lattice gas into the two phase region. Thus the boundary of the two phase region is the natural boundary of the function $p^*(v, \mathcal{J})$.

Appendix A

Method of computation.

Each isotherm of the spherical model of ferromagnetism and of the spherical lattice gas was computed by assigning a value to $\mathcal{J}$ and selecting a set of values for z. For these values $\mathcal{M}, \mathcal{H}$, v, F and p* were computed successively from (55), (56), (12), (15) and (11) using a Burroughs 220 electronic computer. The only difficulty was that of evaluating $f_n(z)$ and $df_n(z)/dz$ for n = 2 and 3. The second term on the right side of (31), which gives df_2/dz, involves the complete elliptic integral of the first kind. This integral also occurs in (39) which gives df_3/dz. It was approximated by a formula of C. Hastings[4, p. 171]. Then df_3/dz was computed by numerical integration using Simpson's one-third rule, which was also used to compute $f_2(z)$ from (36).

The function $f_3(z)$ was computed from the series

$$f_3(z) = \ln z - \frac{3}{4z^2} - \frac{45}{32z^4} - \frac{155}{32z^6} - \frac{22,365}{1,024z^8} - \dots \qquad (A.1)$$

This series can be derived by first writing (47) in the form

$$f_3(z) = \ln z - \sum_{n=1}^{\infty} \frac{A_n}{nz^n} \qquad (A.2)$$

The coefficients in (A.2) are found to be

$$A_n = \frac{1}{\pi^3} \int_0^{\pi}\int_0^{\pi}\int_0^{\pi} \left(\sum_{j=1}^{3} \cos \omega_j \right)^n d\omega_1 d\omega_2 d\omega_3 \; . \qquad (A.3)$$

The integral in (A.3) is expressible in terms of I_o, the modified Bessel function of the first kind of order zero. This yields

$$A_n = \lim_{a\to 0} \frac{d^n}{da^n} \left(\left[I_o(a) \right]^3 \right) \qquad (A.4)$$

Since $I_o(a)$ is an even function of a, it follows from (A.4) that $A_n = 0$ when n is odd. Upon substitution of the power series for I_o into (A.4) we obtain for even n = 2s

$$\frac{A_{2s}}{2s} = \frac{(2s - 1)!}{2^{2s}} \sum_{k=o}^{s} \left[(s-k)! \right]^{-2} \sum_{j=o}^{k} \left[j!(k-j)! \right]^{-2} \qquad (A.5)$$

If A_{2s} is computed for s = 1, 2, 3, 4 from (A.5) and the results are inserted into (A.2), the result is (A.1).

Appendix B

Limit properties of the three-dimensional spherical magnet and the spherical lattice gas.

We shall now prove various statements made in the text about the behavior of the equations of state of the three dimensional spherical models of the magnet and the lattice gas. Let us begin with (41). From (38) it follows that $z \to \infty$ when $\mathcal{J} \to 0$. Then from (38) - (40) we find that as $\mathcal{J} \to 0$,

$$2\mathcal{J} \sim \frac{\mathcal{H}^2}{2\mathcal{J}z^2} + \frac{1}{z} \tag{B.1}$$

$$\mathcal{M} \sim \frac{\mathcal{H}}{2\mathcal{J}z} \quad . \tag{B.2}$$

We now solve (B.1) for $\mathcal{J}z$ and substitute the result into (B.2), which yields (41a).

To prove (41b) we first note from (38) that $z \to 3$ when $\mathcal{J} \to \infty$. We also note that $df_3(3)/dz = 2\mathcal{J}_c$, which was proved by G. N. Watson[5]. Then for $\mathcal{J}$ large, (38) can be written as

$$\left[\frac{\mathcal{H}}{2\mathcal{J}(z-3)}\right]^2 \sim 1 - \frac{\mathcal{J}_c}{\mathcal{J}} \tag{B.3}$$

Thus $\lim\limits_{\mathcal{J}\to\infty} \left[\frac{\mathcal{H}}{2\mathcal{J}(z-3)}\right] = 1$ which completes the proof. To prove (41d) we see from (17) that df_3/dz decreases monotonically from $2\mathcal{J}_c$ at $z = 3$ to zero at $z = \infty$ and that it behaves like z^{-1} for large z. If $\mathcal{J} < \mathcal{J}_c$ and $\mathcal{H} \to 0$, it follows from (38) that $z \to z_m > 3$, where z_m satisfies (C.4), and (41d) follows. If $\mathcal{J} > \mathcal{J}_c$ then $z \to 3$ in (38) when $\mathcal{H} \to 0$ and (38) becomes (B.3), proving (41c). To prove (41e) we observe from (38) that when $\mathcal{H} \to \infty$, $z \to \infty$ and consequently $df_3/dz \to 0$. Then

$$\lim_{\mathcal{H}\to\infty}\left[\frac{\mathcal{H}}{2\mathcal{J}(z-3)}\right] = 1 \quad . \tag{B.4}$$

This is (41e) and completes the proof of (41).

We shall now derive the values of p* in Table 4. When $\mathcal{H} \to \pm\infty$ it follows that $\mathcal{M} \to \pm 1$, since $\mathcal{M}$ is odd. Then from (B.4), $z \sim |\mathcal{H}|/2\mathcal{J} \to \infty$. For large z, $f_3(z) \sim \ln z = \ln |\mathcal{H}|/2\mathcal{J}$. Substitution of these limiting values for z and $f_3(z)$ into (46) as $|\mathcal{H}| \to \infty$ yields

$$F_3 \sim -\frac{1}{2}\ln\frac{|\mathcal{H}|}{2\mathcal{J}} + |\mathcal{H}| \; . \tag{B.5}$$

Substitution of (B.5) into (45) yields, when $\mathcal{H} \to +\infty$, the entry on line 1, column 4 of Table 4. When $\mathcal{H} \to -\infty$ this substitution yields the entry on line 4, column 4 of Table 4. When $\mathcal{H} \to \pm 0$ and $\mathcal{J} < \mathcal{J}_c$, $z \to z_m > 3$ and $H/2\mathcal{J}(z-3) \to 0$. Substitution of these values into (45) yields the entry on line 2, column 4 of Table 4. Finally when $\mathcal{H} \to \pm 0$ and $\mathcal{J} > \mathcal{J}_c$, $z \to z_m = 3$, $\mathcal{H}/2\mathcal{J}(z-3) \to \pm\mathcal{M}(0+, \mathcal{J})$. Again, substituting these values into (45) yields line 3 of Table 4.

Appendix C

Determination of z_m.

We know from (17) that $df_n(z)/dz$ is a positive monotonic decreasing function of z behaving like 1/z for large z. We also know from (24) that $df_1(1)/dz = \infty$, from (31) that $df_2(2)/dz = \infty$ and from Appendix B that $df_3(3)/dz = 2\mathcal{J}_c$. Therefore z_m corresponds to the smallest non-negative value of $\mathcal{M}^2$ that can be realized from (55). For n = 1, 2 and all $\mathcal{J}$ and for n = 3, $\mathcal{J} < \mathcal{J}_c$ this is $\mathcal{M}^2 = 0$. Hence under these condtions, z_m is a solution of

$$\frac{df_n(z_m)}{dz} = 2\mathcal{J} \; . \qquad (C.1)$$

More specifically

$$z_m = \left(1 + \frac{1}{4\mathcal{J}^2}\right)^{1/2} \qquad n = 1 \qquad (C.2)$$

$$z_m = \frac{1}{\pi\mathcal{J}} \; K\left(\frac{2}{z_m}\right) \qquad n = 2 \qquad (C.3)$$

$$\frac{df_3(z_m)}{dz} = 2\mathcal{J} \qquad n = 3, \; \mathcal{J} < \mathcal{J}_c \; . \qquad (C.4)$$

From Appendix B we also have

$$z_m = 3 \qquad n = 3, \; \mathcal{J} > \mathcal{J}_c \; . \qquad (C.5)$$

In all cases $z_m \geq n$.

Appendix D

Shapes of the isotherms of the spherical lattice gas.

The slope of the isotherms of the spherical lattice gas can be expressed simply in terms of the properties of the spherical model of a ferromagnet. To show this we differentiate (11) with respect to v and (12) with respect to $\mathcal{H}$. Upon combining these two equations we obtain, after use of (14),

$$\frac{dp^*}{dv} = - \frac{(1+\mathcal{M})^3}{2\mathcal{J} \; \frac{d\mathcal{M}}{d\mathcal{H}}} \; . \qquad (D.1)$$

This relationship also relates the ordinary lattice gas and the Ising model.

Let us now evaluate $d\mathcal{M}/d\mathcal{H}$ for the spherical model. To do so we differentiate (18) and (16) with respect to $\mathcal{H}$ and combine the two results. We then obtain for the spherical magnet

$$\frac{d\mathcal{M}}{d\mathcal{H}} = \frac{1}{2\mathcal{J}(z-n)} \left\{ \frac{-\dfrac{d^2 f_n}{dz^2}}{\dfrac{4\mathcal{J}\mathcal{M}^2}{(z-n)} - \dfrac{d^2 f_n}{dz^2}} \right\} . \tag{D.2}$$

Since $\frac{d^2 f_n}{dz^2} \leq 0$ it follows from (D.2) that $\frac{d\mathcal{M}}{d\mathcal{H}} \geq 0$ and from (D.1) that

$\frac{dp^*}{dv} \leq 0$.

Let us now deduce (42) - (44), (53) and (54). If $\mathcal{J} = 0$, (42) follows directly from (41a). For $\mathcal{J} > 0$ we have for $z \sim 3$ [2, p. 385]

$$\frac{d^2 f_3(z)}{dz^2} \sim -\left[2^{3/2}\,\pi\,(z-3)^{1/2}\right]^{-1} . \tag{D.3}$$

From this equation and (17) it follows that $\frac{d^2 f_3(z)}{dz^2}$ increases monotonically from $-\infty$ at $z = 3$ to zero at $z = \infty$.

If $0 < \mathcal{J} < \mathcal{J}_c$ then, as is shown in Appendix C, when $\mathcal{H} \to 0$ it follows that $z \to z_m > 3$ and $\mathcal{M} \to 0$. Hence $d^2 f_3(z)/dz^2 \to d^2 f_3(z_m)/dz^2 \neq 0$. Upon substitution into (D.2) of the limits attained by z, $\mathcal{M}$ and $d^2 f_3(z)/dz^2$ as $\mathcal{H} \to 0$ we obtain (43). If $\mathcal{J} > \mathcal{J}_c$ then from Appendix C we find that as $\mathcal{H} \to 0$, $z \to 3$ and $\mathcal{M}^2 \to (1 - \mathcal{J}_c/\mathcal{J}) > 0$. Hence from (D.3), $d^2 f_3/dz^2 \to -\left[2^{3/2}\pi\,(z-3)^{1/2}\right]^{-1}$. Substitution of these limiting values of z, $\mathcal{M}$ and $d^2 f_3(z)/dz^2$ into (D.2) yields (44).

Equation (53) then follows upon substitution of (41d) and (43) into (D.1), and (54) follows upon substitution of (41c) and (44) into (D.1).

References

[1] Yang, C.N. and Lee, T.D. - Phys. Rev. 87, 410-419(1952).

[2] Berlin, T.H. and Kac, M. - Phys. Rev. 86, 821-835(1952).

[3] Newell, G.F. and Montroll, E.W. - Rev. Mod. Phys. 25, (353-389)1953.

[4] Hastings, C., Jr. - Approximations For Digital Computers, Princeton University Press, 1955, p. 171.

[5] Watson, G.N. - Quart. Jour. Math. 10, 266(1939).

DISTRIBUTION LIST FOR RESEARCH REPORTS

Contract No. AF 49(638)-341

(ONE copy unless otherwise noted)

(10) Commander
Air Force Office of Scientific Research
Air Research and Development Command
ATTN: SRY
Washington 25, D.C.

(4) Commander
Wright Air Development Center
ATTN: WCOSI-3
Wright-Patterson Air Force Base, Ohio

Commander
Air Force Cambridge Research Center
ATTN: Technical Library
L.G. Hanscom Field
Bedford, Mass.

Commander
Rome Air Development Center
ATTN: RCSST-4
Griffiss Air Force Base
Rome, N.Y.

Director, Office for Advanced Studies
Air Force Office of Scientific Research
Air Research and Development Command
P.O. Box 2035
Pasadena 2, California

(2) Commander
European Office
Air Research and Development Command
47 rue Cantersteen
Brussels, Belgium

(10) Commander
ASTIA
ATTN: TIPDR
Arlington Hall Station
Arlington 12, Virginia

Director of Research and Development
Headquarters USAF
ATTN: AFDRD
Washington 25, D.C.

Chief of Naval Research
Department of the Navy
ATTN: Code 420
Washington 25, D.C.

Director, Naval Research Laboratory
ATTN: Technical Information Officer
Washington 25, D.C.

Director, Research and Development Division
General Staff
Department of the Army
Washington 25, D.C.

Chief, Physics Branch, Division of Research
U.S. Atomic Energy Commission
1901 Constitution Ave., N.W.
Washington 25, D.C.

U.S. Atomic Energy Commission
Technical Information Extension
P.O. Box 62
Oak Ridge, Tennessee

National Bureau of Standards Library
Room 203, Northwest Building
Washington 25, D.C.

National Science Foundation
1520 H Street, N.W.
Washington 25, D.C.

Director, Office of Ordnance Research
Box CM, Duke Station
Durham, North Carolina

Office of Technical Services
Department of Commerce
Washington 25, D.C.

Commander
Arnold Engineering Development Center
Tullahoma, Tennessee
ATTN: Technical Library

Commander
Air Force Armament Center
Eglin Air Force Base, Florida
ATTN: Technical Library

Commander
Air Force Flight Test Center
U.S. Air Force
ATTN: FTOTL
Edwards Air Force Base, California

Commander
Air Force Missile Test Center
ATTN: Technical Library
Patrick Air Force Base
Cocoa, Florida

Commander
Air Force Special Weapons Center
ATTN: Technical Library
Kirtland Air Force Base, New Mexico

Commander
Air Force Missile Development Center
ATTN: Technical Library
Holloman Air Force Base, New Mexico

Commander
Air Force Cambridge Research Center
ATTN: CROOTR
L.G. Hanscom Field
Bedford, Mass.

Commander
Army Rocket and Guided Missile Agency
Redstone Arsenal
ATTN: ORDXR-CTL
Alabama

Commandant
Air Force Institute of Technology
ATTN: MCLI, Technical Library
Wright-Patterson Air Force Base, Ohio

Commander
Air Force Ballistic Missile Div., HQ, ARDC
ATTN: WDSOT
P.O. Box 262
Inglewood, California

Applied Mechanics Review
Southwest Research Institute
8500 Culebra Rd.
San Antonio, Texas

Institute of the Aeronautical Sciences
ATTN: Librarian
2 E. 64th St.
New York 16, N.Y.

Date Due

MAY 2 1975

PRINTED IN U. S. A.

NYU
HT-
5
c.1

NYU
HT-
5 Pressman
c.1

NYU
HT-
5 Pressman
c.1

AUTHOR
Equation of state and phase
TITLE transition of the
spherical lattice gas

DATE DUE	BORROWER'S NAME	ROOM NUMBER
~~AY 2~~	~~Bellelsen Dabst~~	

N. Y. U. Institute of
Mathematical Sciences
25 Waverly Place
New York 3, N. Y.

NEW YORK UNIVERSITY
INSTITUTE OF MATHE[illegible] SCIENCES
[illegible]
Pl.